18th International Conference on Structure Mechanics in Reactor Technology (SMiRT 18)
Beijing, China, August 7-12, 2005
SMiRT18-J05-4

EXPERIMENTAL STUDY ON BEHAVIOR OF RC PANELS COVERED WITH STEEL PLATES SUBJECTED TO MISSILE IMPACT

Jun Hashimoto*
Tokyo Institute of Technology
2-12-1, O-okayama, Meguro-ku, Tokyo, Japan, 152-8552
Phone: +81-3-5734-3155
Fax: +81-3-5734-3155
e-mail: jhashimo@tm.mei.titech.ac.jp

Katsuki Takiguchi, Koshiro Nishimura, Kazuyuki Matsuzawa, Mayuko Tsutsui
Tokyo Institute of Technology

Yasuhiro Ohashi, Isao Kojima, Haruhiko Torita
Shimizu Corporation

ABSTRACT

This paper describes an experimental study on the behavior of concrete panels with steel plate subjected to missile impact. Two tests were carried out, divided in accordance with the types of projectile, non-deformable and deformable. In all, 40 specimens of 750mm square were prepared. The panel specimen was suspended vertically by two steel wire ropes to allow free movement after projectile impact, and was subjected to a projectile. As a result, it is confirmed that a RC panel with steel plate on its back side has higher impact resistance performance than a RC panel and that thickness of concrete panel, thickness of steel plate and the impact velocity of the projectile have a great effect on the failure modes of steel concrete panels. Moreover, based on the experimental results, the quantitative evaluation method for impact resistance performance of RC panels covered with steel plates is examined. The formula for perforation velocity of a half steel concrete panel, proposed in accordance with the bulging height, is effective to evaluate the impact resistance performance of RC panels with steel plates.

Keywords: missile impact, concrete, steel plate, non-deformable projectile, deformable projectile

1. INTRODUCTION

The necessity to design nuclear-related facilities for an extreme load condition, such as an accidental aircraft crash or unexpected terrorist attack, is well recognized for their social importance, since an unexpected extreme load would results in both local and overall dynamic response of the target wall. A reinforced concrete panel has usually been used with the nuclear-related facilities, and several methods to improve damage resistance of reinforced concrete panels have been recommended. Many studies have been conducted on the resistance of reinforced concrete panels subjected to missile impact. As for the local damage of reinforced concrete panel, several formulae were proposed for thickness of a reinforced concrete panel needed for perforation or scabbing on its rear face. [1]-[4]

Meanwhile, steel plate reinforced concrete, which was developed recently, is expected to be a good impact resistance structure, since it is effective in preventing a projectile from perforating the walls due to steel plates covering the concrete surface. Moreover, the decrease of thickness of a wall or a roof and the rationalization of structure can be expected by applying steel plate reinforced concrete to a building. However, experimental research is needed and to obtain more data in order to evaluate the impact resistance performance of reinforced concrete panels with steel plates.

In this research, experimental study on the behavior of RC panels reinforced with steel plates subjected to missile impact was carried out. The objectives of this experiment are to understand the effect of reinforcement with steel plate on the local damage of RC panel due to missile impact and to propose the method to evaluate the local damage of RC panels reinforced with steel plates.

2. TEST PROGRAM

Two tests were carried out to provide insight into the behavior of RC panel under projectile impact using non-deformable and deformable projectiles in Test 1 and Test 2, respectively. The parameters studied include thickness of RC panel, thickness of steel plate, velocity of projectile, and rigidity of projectile.

2.1 Specimens and Materials

In all, 40 specimens were tested in this study. The specimens were divided into three series: RC, HSC and SC. The specimens in series RC were prepared as control specimens. Series HSC consisted of half steel plate reinforced concrete panels, which comprise concrete panels with reinforcing bars on front side and steel plate on rear side. Meanwhile, the specimens in series SC were steel plate reinforced panels, which consist of concrete panels with steel plates on both sides. The details of specimens are shown in Figure 1. All specimens in series RC and HSC were reinforced with deformed bars of 6.35mm diameter at spacing of 100mm. In series HSC and SC, the steel plates of 750mm square were fixed on the surface of RC panels with stud bolts (M3) (see Figure 1 (b) and (c)). Here, the spacing of stud bolts was 50mm. With all specimens used in this experiment, the target compressive strength of the concrete used in this experiment is 30Mpa. A coarse aggregate with maximum size of 10mm was used. The properties of materials used in this study are shown in Table 1.

In Test 1, eight RC panels, 16 HSC panels and four SC panels were prepared. These specimens, all of 750mm square, were prepared with five different thicknesses; 60mm, 80mm, 100mm, 120mm and 150mm. The thicknesses of steel plate used with specimens in series HSC and SC were 0.5mm, 0.8mm, and 1.2mm. In Test 2, four RC panels and 8 HSC panels were prepared with thickness of 80mm. With specimens in series HSC, steel plates with two different thicknesses of 0.5mm and 0.8mm were used.

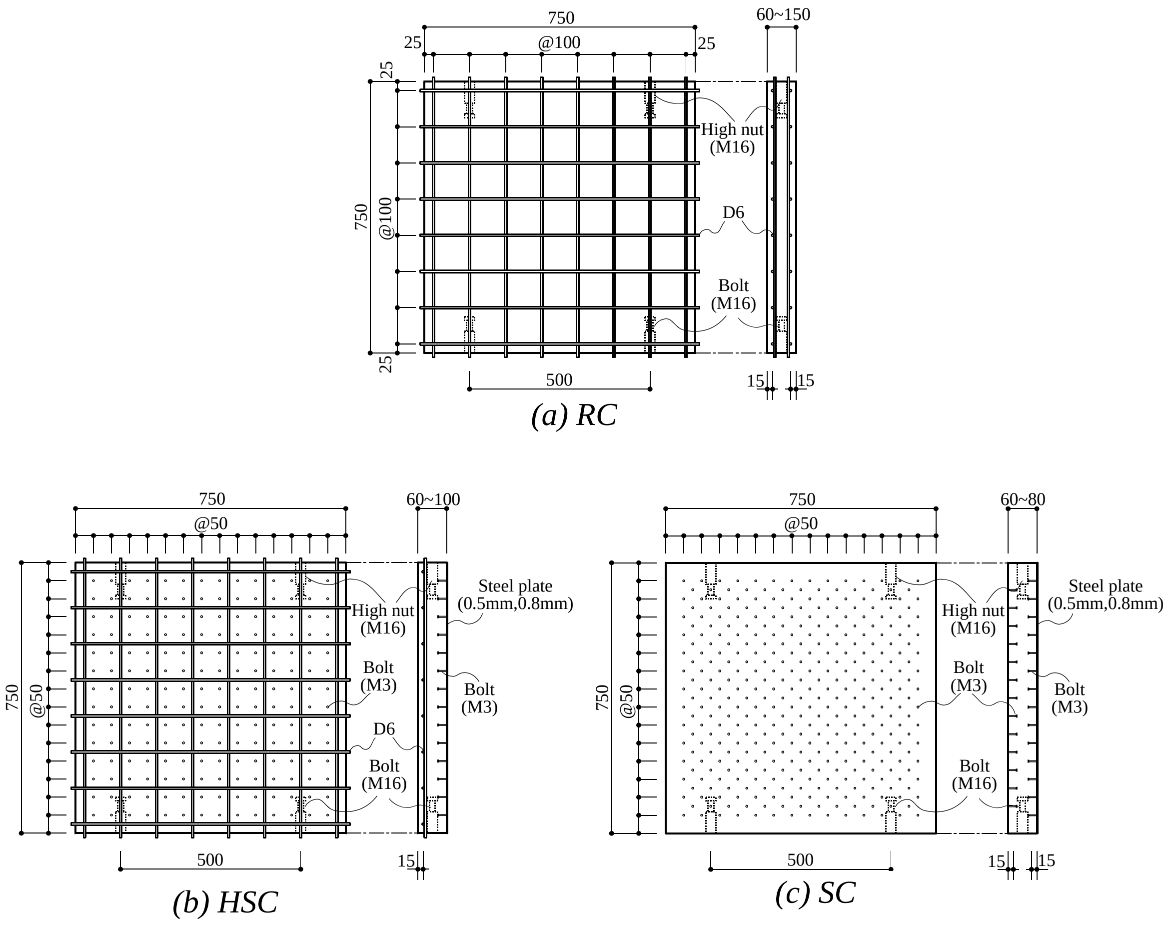

Fig.1 – Detail of the specimens

Table 1 – Material properties

	Steel Plate		Deformed steel bar	Concrete	
	Thickness (mm)	Tensile strength (MPa)	Tensile strength (MPa)	Compressive strength (MPa)	Splitting tensile strength (MPa)
Test 1	0.5	326	472	28.7	2.53
	0.8	303			
	1.2	330			
Test 2	0.5	352	606	28.3	2.30
	0.8	498			

2.3 Test Setup and Instrumentation

In this study, one type of non-deformable projectile and three types of deformable projectile were used. The details of the projectiles are shown in Figure 2. All types of projectiles, with a mass of about 0.5kg and diameter of 45mm, have a spherical head made of steel. The deformable projectiles have a hollow section, and were designed with different materials and forms to vary the way of deformation. This projectile was ejected by air pressure at a target velocity. In this experiment, the target velocities were decided in the range of 140m/sec to 270m/sec. Velocity of the projectiles was measured by three methods; 1) an electro-optical device, 2) a high speed camera, and 3) a high-speed analog voltmeter. (Refer to [5] for detail.)

The panel specimen was suspended vertically in front of the gun by two steel strings to allow free movement after impact (see Figure 3). After testing, the weight of breaking off concrete debris of all specimens was measured. The dimension of the damaged area of both front and rear faces of the RC panels was examined. The dimension of damage area of front faces of the HSC panels and the bulging height of HSC and SC specimens was also taken. Moreover, the deformation of deformable projectile after impact was measured.

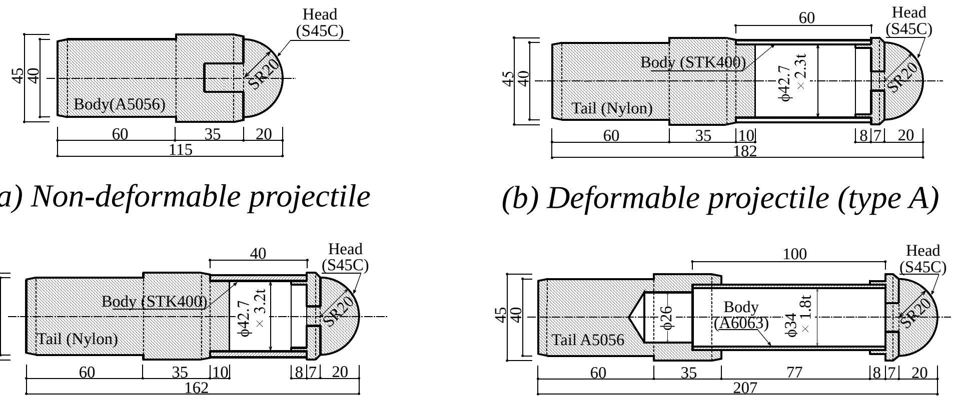

(a) Non-deformable projectile *(b) Deformable projectile (type A)*

(c) Deformable projectile (type B) *(d) Deformable projectile (type C)*

Fig. 2 – Missile projectile

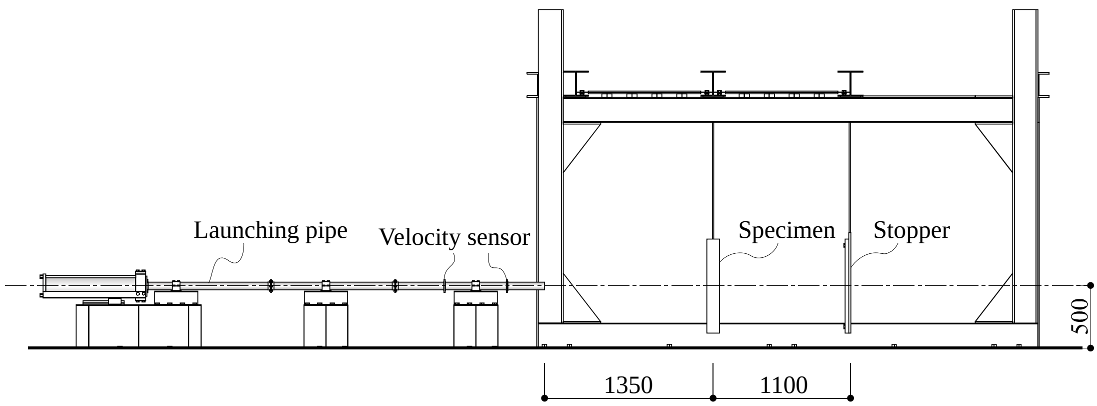

Fig. 3 – Test setup

3. TEST RESULTS AND DISCUSSION

3.1 EXPERIMENT RESULTS

The test results with parameters studied in this experiment are presented in Table 2. Here, the types of the failure mode of specimens are divided as shown in Figure 4. Based on both measurements taken using the three methods previously mentioned and calculation based on theoretical formula, the velocities of missile projectile were decided. (Refer to [5] for detail.) Figure 5 and Figure 6 shows the representative failure conditions of the tested specimens. Figure 7 shows a state of failure of the specimen in series HSC taken with a high-speed camera, which is capable of recording 10000 frames per second.

Table 2 – Test results

(a) Test 1 (Non-deformable type of projectile)

Specimen			Steel plate (Reinforcement)		Target velocity (m/sec)	Test results				
Series	Name	Thickness (mm)	Thickness (mm) Front face	Thickness (mm) Rear face		Failure mode	Weight of concrete debris (kgf)	Area of damage area (cm^2) Front face	Area of damage area (cm^2) Rear face	Bulging Height (mm)
RC	RC-N-1	60			175	Perforation	1.93	104	284	
	RC-N-2	80			175	Perforation	2.40	133	401	
	RC-N-3	100			175	Scabbing	4.90	204	860	
	RC-N-4	100			215	Perforation	3.75	340	670	
	RC-N-5*1	100			215	Perforation	3.00	263	394	
	RC-N-6	120			215	Scabbing	4.34	209	1213	
	RC-N-7	120			250	Perforation	5.30	305	1372	
	RC-N-8	150			250	Penetration	1.80	387	0	
HSC	HSC-N-1	60		0.5	140	Splitting	0.79	88		-
	HSC-N-2	80			140	Bulging	0.45	99		18.8
	HSC-N-3	60			175	Perforation	1.20	99		-
	HSC-N-4	80			175	Bulging	0.60	216		34.2
	HSC-N-5	80			215	Perforation	1.70	204		-
	HSC-N-6	100			250	Bulging	1.23	227		43.8
	HSC-N-7	60		0.8	175	Bulging	1.18	99		47.7
	HSC-N-8*2	60			175	Bulging	0.88	123		57.8
	HSC-N-9*3	80			175	Bulging	0.64	139		28.3
	HSC-N-10	60			215	Perforation	0.76	135		-
	HSC-N-11	80			215	Bulging	0.55	161		43.5
	HSC-N-12	80			250	Perforation	1.60	222		-
	HSC-N-13	100			250	Bulging	1.85	401		34.3
	HSC-N-14	80		1.2	175	Bulging	0.55	121		18.5
	HSC-N-15	80			215	Bulging	0.86	167		34.2
	HSC-N-16	80			250	Splitting	0.90	186		53.8
SC	SC-N-1	60	0.8	0.8	175	Bulging	0.18			44
	SC-N-2	60			175	Bulging	0.13			44.7
	SC-N-3	80			250	Splitting	0.55			-
	SC-N-4	60	1.2	1.2	175	Bulging	0.08			32.8

*1 Deformed bars (D3) for spreaders were used.
*2 The spacing of stud bolts (M3) was 100mm, and a stud bolt was arranged at the center of specimen.
*3 The spacing of stud bolts (M3) was 100mm.

(b) Test 2 (Deformable type of projectile)

Specimen			Steel plate (Reinforcement)		Type of deformable projectile	Target velocity (m/sec)	Test results					
Series	Name	Thickness (mm)	Thickness (mm) Front face	Thickness (mm) Rear face			Failure mode	Weight of concrete debris (kgf)	Area of damage area (cm^2) Front face	Area of damage area (cm^2) Rear face	Bulging Height (mm)	Deformation of projectile (mm)
RC	RC-D-1	80			A	215	Perforation	3.85	282	349		-
	RC-D-2				B	175	Perforation	2.85	135	365		-
	RC-D-3				C	175	Scabbing	4.50	137	625		70.5
	RC-D-4				C	215	Perforation	4.60	127	399		73.5
HSC	HSC-D-1	80		0.5	C	175	Bulging	1.00	75		3.60	46.30
	HSC-D-2				C	215	Splitting	1.45	123		-	70.50
	HSC-D-3				C	250	Perforation	2.05	143		-	71.70
	HSC-D-4			0.8	C	175	Bulging	1.10	116		13.85	67.80
	HSC-D-5				C	215	Bulging	1.05	174		30.40	71.10
	HSC-D-6				C	250	Bulging	1.30	142		43.80	77.10
	HSC-D-7				C	260	Bulging	1.60	222		47.20	80.70
	HSC-D-8				C	270	Bulging	1.55	146		51.00	81.40

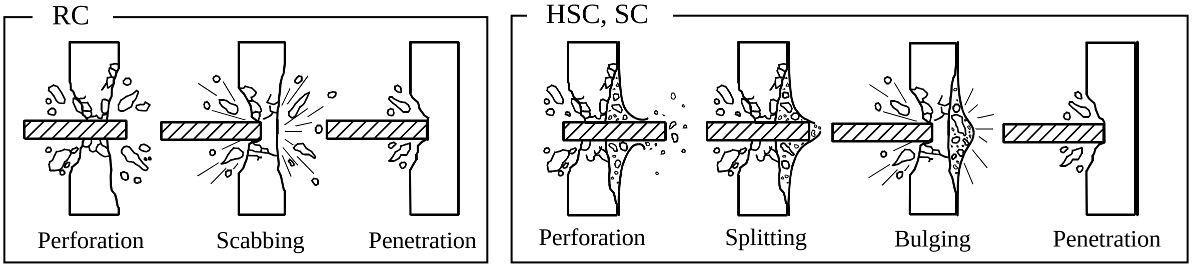

Fig.4 – Failure mode

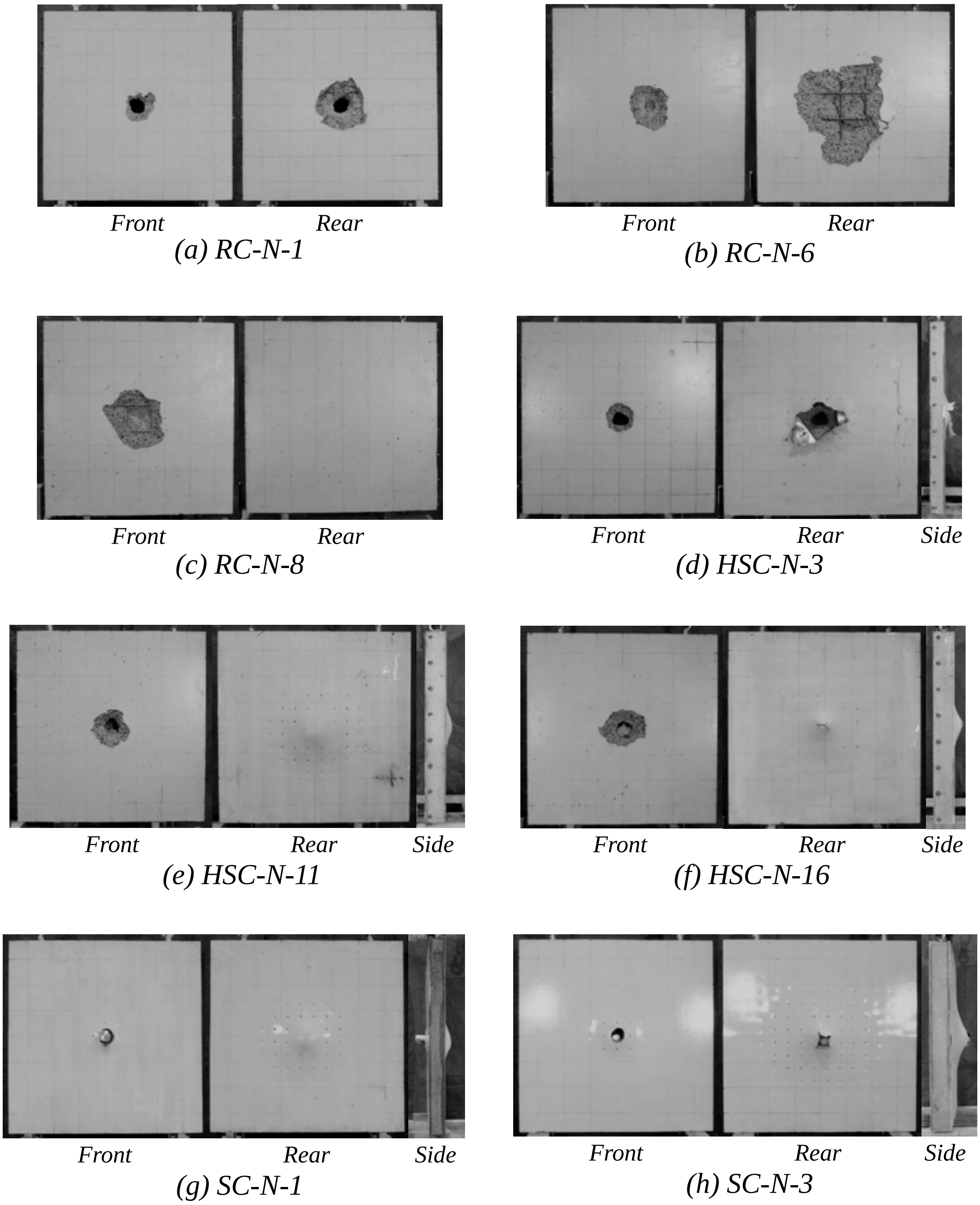

Fig.5 – Damages of specimens subjected to non-deformable projectile

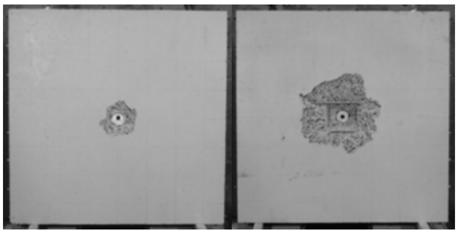

Front *Rear*

(a) RC-D-3

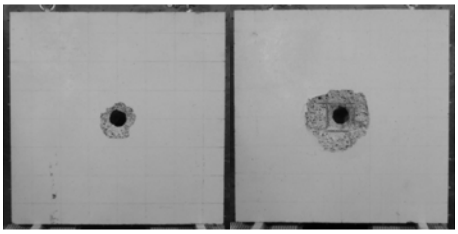

Front *Rear*

(b) RC-D-4

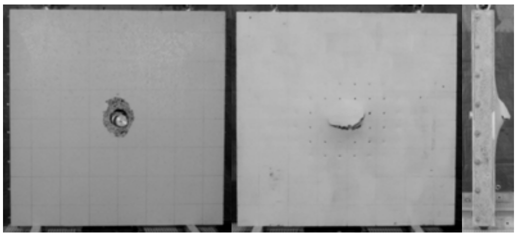

Front *Rear* *Side*

(c) HSC-D-2

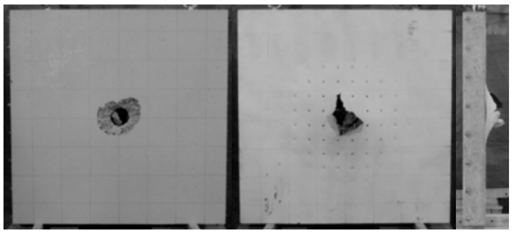

Front *Rear* *Side*

(d) HSC-D-3

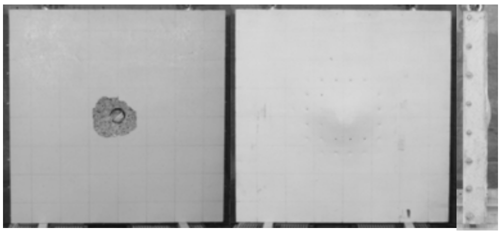

Front *Rear* *Side*

(e) HSC-D-5

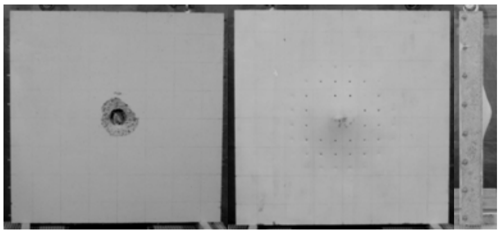

Front *Rear* *Side*

(f) HSC-D-8

Fig.6 – Damages of specimens subjected to deformable projectile

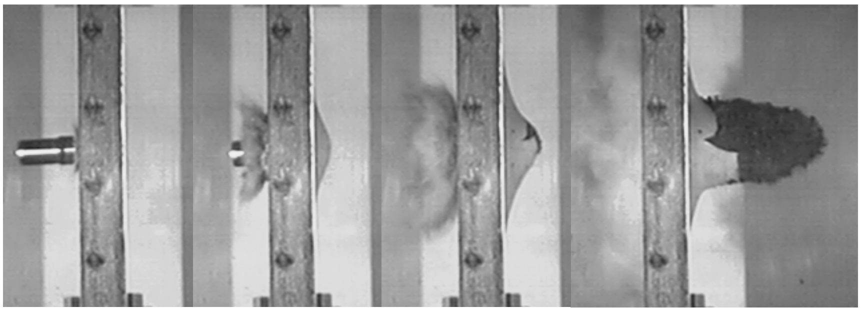

Fig.7 – State of failure

<u>Results of test with non-deformable projectile</u>

Test results of Test1 are presented in Table 2 (a). Comparison of failure mode by experimental parameters is shown in Table 3. With all types of specimens, the greater the thickness of the concrete panel and the lower the velocity of the projectile, the smaller the degree of damage. Furthermore, specifically for HSC, thicker steel plates also result in less local damage. With regards to bulging height, thicker steel plates and concrete panels combined with a slower projectile result in less local damage. Therefore, it is supposed that the thickness of the steel plates and concrete panels and missile velocity have a great effect on the mode of failure which occurs.

Compared with specimens with a thickness of 80mm, which were tested with velocity of 175m/s, the specimens in series RC failed in the perforation mode, while the specimens in series HSC failed in the bulging mode. These results show that steel concrete panels are superior to reinforced concrete panels with regard to impact resistance. However, there is little difference in failure modes and bulging height between specimens in

Table 3 – Comparison of failure mode in Test 1

Specimen		RC			HSC										SC		
Thickness of steel plate (mm)		-			0.5				0.8			1.2			0.8		1.2
Velocity of projectile (m/sec)		175	215	250	140	175	215	250	175	215	250	175	215	250	175	250	175
thickness of concrete panel (mm)	60	×			△	×			□	×					□		
	80	×			□	□	×			□	×	□	□	△		△	
	100	△	×					□			□						
	120		△	×	×: Perforation △: Scabbing/Splitting □ : Bulging ○: Penetration												
	150			○													

Table 4 – Comparison of failure mode by type of projectile

Specimen	Thickness of steel plate (mm)	Thickness of concrete panel (mm)	Type of projectile	Velocity of projectile (m/sec)					
				140	175	215	250	260	270
RC	/	80	Non-deformable		×				
			Deformable A			×			
			Deformable B		×				
			Deformable C		△	×			
HSC	0.5		Non-deformable	□	□	×			
			Deformable C		□	△	×		
	0.8		Non-deformable			□	×		
			Deformable C		□	□	□	□	□

× : Perforation △: Scabbing/Splitting □: Bulging

Fig.8 – Condition of deformable projectile after impact

series SC and HSC when tested under the same experimental condition. Consequently, a steel plate on the front face of a concrete panel is less effective in impact resistance than a steel plate on the rear face.

<u>Results of test with deformable projectile</u>

Test results of Test 2 are shown in Table 2 (b). With HSC-D-1, the projectile failed to load and the damage of the specimen obviously differed from other specimens. Hence, the result of this specimen was excluded from the discussion. Compared with the deformable projectile type A and B, which bodies were hardly deformed after impact, the projectiles of deformable type C were deformed like bellows (see Figure 5). Furthermore, the RC specimen subjected to a non-deformable projectile and deformable projectile type B with velocity of 175m/s failed in the perforation mode, while the RC specimen tested by deformable type C projectile with the same velocity failed in the scabbing mode (see Table 4). These results show that the deformable projectile type C could absorb enough energy, and this projectile was used in test of HSC to compare the results of test with a non-deformable projectile.

The deformable projectile type C to which the HSC specimens were subjected was also deformed and it is found that the projectile absorbed the energy by its deformation. The deformable projectile did not perforate the specimens in series HSC, with the same velocity of non-deformable projectile which perforated the specimens in series RC (See Table 4). Moreover, the bulging height of HSC specimen tested by deformable projectile was lower than that by non-deformable projectile. Therefore, the degree of damage by impact of deformable projectile was smaller than that of a non-deformable projectile when the specimens were subjected to the same velocity of impact.

3.2 RELATIONSHIP BETWEEN BULGING HEIGHT AND IMPACT VELOCITY

In this study, an attempt was made to develop a method for quantitative evaluation of the relationship between bulging height of a steel plate on rear face of a HSC specimen and velocity of the non-deformable missile projectile.

The kinetic energy of a projectile is absorbed by concrete. However, in the case of impact by the projectile with velocity over scabbing velocity, the energy that cannot be absorbed by concrete is consumed by crushing concrete or breaking off concrete debris as kinetic energy. It is supposed that this energy is finally consumed by the deformation of the steel plate, and the energy consumption of steel plate E_s (J) is expressed as following:

$$E_s = \frac{1}{2} m \left(v^2 - v_s^2\right) \qquad \text{Eq. (1)}$$

where, m is the mass of projectile (kg), v is the impact velocity (m/sec), and v_s is the scabbing velocity (m/sec).

Regarding the area of steel plate affected by energy consumption, the impact force transmits through concrete with spreading and influences the steel plate. Based on the assumption of a collapse mechanism like shear corn failure shown in Figure 9, the area of steel plate suffering impact force A_{SE} (mm^2) can be written as:

$$A_{SE} = \pi \left(t + \frac{d}{2} \right)^2 \qquad \text{Eq. (2)}$$

where, t is the thickness of the RC panel (mm), and d is the diameter of projectile (mm). Therefore, energy consumption per unit area that subjected to impact force E (J/mm^2) is following:

$$E = \frac{E_s}{A_{SE}} = \frac{m\left(v^2 - v_s^2\right)}{2\pi\left(t + \frac{d}{2}\right)^2} \qquad \text{Eq. (3)}$$

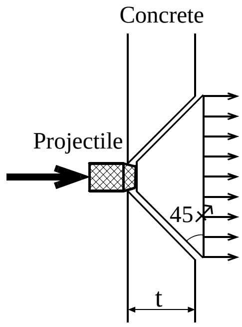

Fig.9 – Assumption of collapse mechanism

Figure 10 shows the relationship between energy consumption per unit area that subjected to impact force E (J/mm^2) and bulging height H (mm). Here, the scabbing velocity by Chang's formula[1)] is expressed as $v_s = v_s(t)$, and $v_s(0.8t)$ which is revised to adjust to the test results, was used for evaluation in this paper. The compressive strength of concrete of 30Mpa is used. It can be found that the bulging height H is in proportional to the energy consumption E in each thickness of steel plate.

$$E = \frac{E_s}{A_{SE}} = \alpha H \qquad \text{Eq. (4)}$$

where, α is the coefficient of energy consumption for the steel plate. The gradients of the straight lines in Figure 10 are reciprocal of α, and it is also observed from Figure 10 that the greater the thickness of a steel plate, the smaller the slopes of the straight lines. In other words, it is supposed that α is a function of the thickness of the steel plate T (mm). Figure 11 shows the relationship between α obtained by straight-line approximations which passes through the origin of the coordinates and thickness of steel plate T, and the following equation is applied by the approximation of the test results.

$$a = \frac{\sqrt{T}}{144.4} \qquad \text{Eq. (5)}$$

Using Equation (1), (3), (4) and (5), impact velocity can be expressed as following;

$$v^2 = \frac{\sqrt{T}}{144.4} \cdot \frac{2\pi}{m} \cdot H \left(t + \frac{d}{2} \right)^2 + v_s^2 \qquad \text{Eq. (6)}$$

Here, in this paper, $v_s(0.8t)$ by Chang's formula was used as the scabbing velocity.

In this experiment, HSC-N-12 failed in the splitting mode, with small crack in the steel plate of the rear face. Based on the assumption that the bulging height of this specimen, 53.8mm, is the critical bulging height which splitting occurs, splitting velocity can be evaluated by substituting 53.8mm for H of Equation (7). The comparison between the test results of HSC and SC and the evaluation equation is shown in Figure 12. From these figures, it can be seen that the result of the evaluation by Equation (6) based on the assumption that the critical bulging height H is 53.8mm accurately expresses the experimental results.

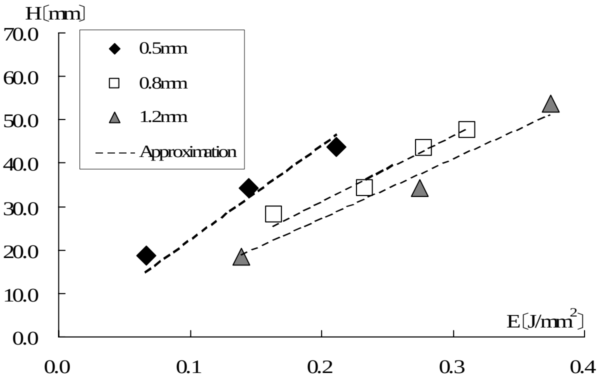

Fig.10 – Relation between energy consumption and bulging height

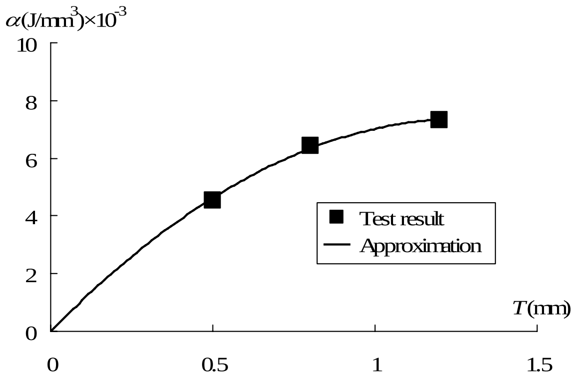

Fig.11 – Relation between thickness of steel plate and coefficient of energy consumption

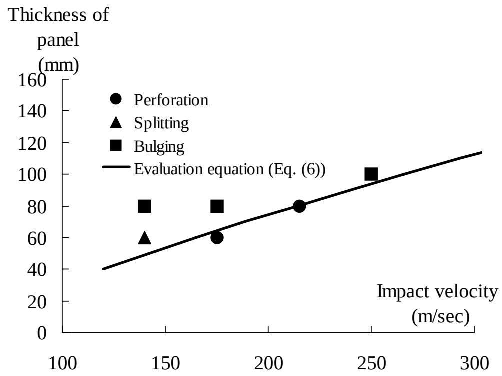

(a) Thickness of steel plate T=0.5mm

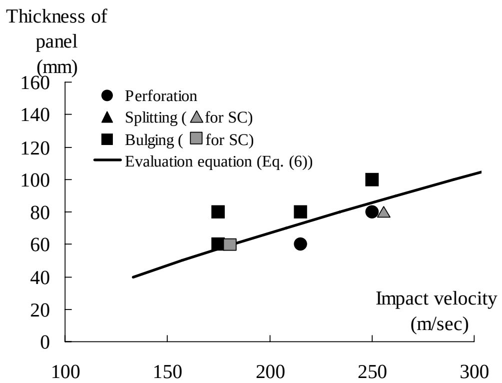

(b) Thickness of steel plate T=0.8mm

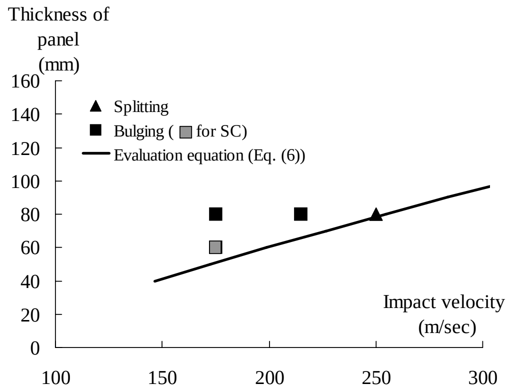

(c) Thickness of steel plate T=1.2mm

Fig.12 – Relation between impact velocity and thickness of panel

3.3 INFLUENCE OF ABSORBED ENERGY OF DEFORMABLE PROJECTILE

The local damage of specimens subjected to deformable projectiles is smaller than that of non-deformable projectiles, and cannot be evaluated by using the same evaluation equation for non-deformable projectiles. However, it is supposed that kinetic energy of non-deformable projectiles is equivalent to the value obtained by subtracting absorbed energy by the deformation of deformable projectile from the total kinetic energy of the deformable projectile, and that the local damage of the specimens subjected to the deformable projectile can be evaluated using the same evaluation equation used for non-deformable projectile.

To obtain data for determining the absorbed energy by deformation of a projectile, compression tests of deformable projectile type C were carried out. The test results are shown in Figure 13. Figure 14 indicates the

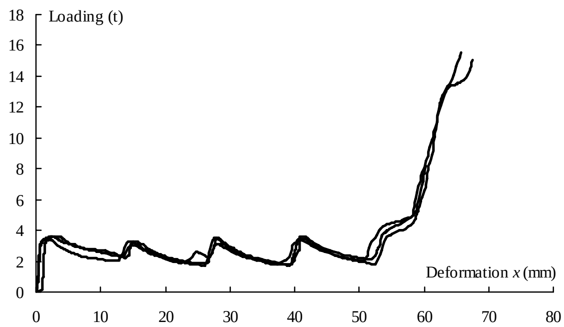

Fig.13 – Result of compression test of deformable projectile

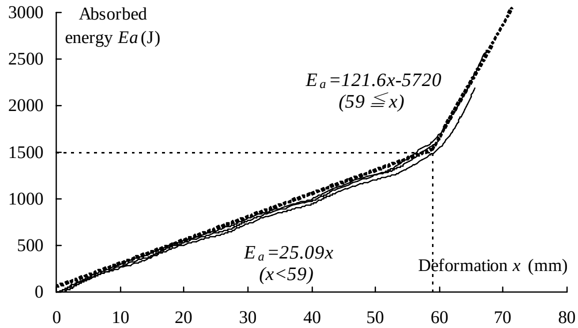

Fig.14 – Relation between deformation and absorbed energy

Fig.15 – Projectile after compression test

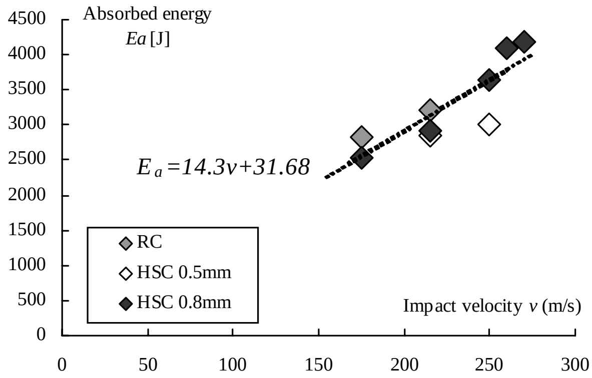

Fig.16 – Absorbed energy of deformable projectile by impact

relationship between the deformation and absorbed energy of the deformable projectile. The test specimen was the deformable projectile (type C) which head had been removed. In the early stages in which the loading increases and decreases, the body of projectiles made of aluminum was deformed like bellows (see Figure 15). After this, the loading increased rapidly, and the rate of increase of the absorbed energy to the deformation changed. Therefore, the relation of absorbed energy and deformation of projectile was approximated by two straight lines (see Figure 14).

$$E_a = 25.09x \qquad (x < 59)$$
$$E_a = 121.6x - 5720 \qquad (x \geq 59) \qquad \text{Eq. (8)}$$

Here, E_a is the absorbed energy of projectile (J), and x is deformation (mm). After the deformation of the projectile reached 70mm, the loading could not continue, and it is assumed that the increase of absorbed energy is the same with that that of the later stages of loading.

With each specimen subjected to deformable projectile (type C), the absorbed energy of projectile was decided by substitution of the deformation of deformable projectile (type C) measured after impact for Equation (8). The relationship between this absorbed energy and the velocity of the deformable projectile is shown in Figure 16, and modeled with the following:

$$E_a = E_a(v) = 14.3v + 31.68 \qquad \text{Eq. (9)}$$

Here, v is an impact velocity of projectile (m/sec), and this relationship is applied within the range of experimental conditions (the velocity of projectile 175-270m/sec, the thickness of concrete panel 80mm). With all types of specimen, the higher the velocity of projectile, the bigger the absorbed energy.

The equivalent kinetic energy of deformable projectile E_v' (J) can be given by following:

$$E_v' = E_v - E_a \qquad \text{Eq. (10)}$$

Here, E_v is the kinetic energy of projectile (J). In the case of non-deformable projectile, E_a is 0(J), and this equivalent kinetic energy does not depend on type of projectile.

Considering Equation (10) for the RC specimens, it is examined that the perforation velocity of a deformable projectile (type C) v_p (m/sec) can be evaluated with the same evaluation equation as a non-deformable projectile. In this paper, the perforation velocity by Chang's formula[1)] is expressed by $v_p = v_p(t)$. Here, $v_p(1.2t)$, which is a revised value to adjust to the experimental results of non-deformable projectile by multiplying a thickness of concrete panel t by revision rate 1.2, is used for evaluation.

In Figure 17, the relationship between the equivalent impact velocity of projectiles and thickness of concrete panels is shown. The equivalent impact velocity v' can be expressed as following using the equivalent kinetic energy E_v':

$$v' = \sqrt{\frac{2E_v'}{m}} \qquad \text{Eq. (11)}$$

RC-D-3, which was subjected to the deformable projectile (type C) with velocity of 175m/sec, failed in the scabbing mode, but it was judged from the failure condition of that it was nearly at perforation limit. It is found in Figure 17 that the result of this specimen can quite accurately be evaluated with using $v_p = v_p(1.2t)$.

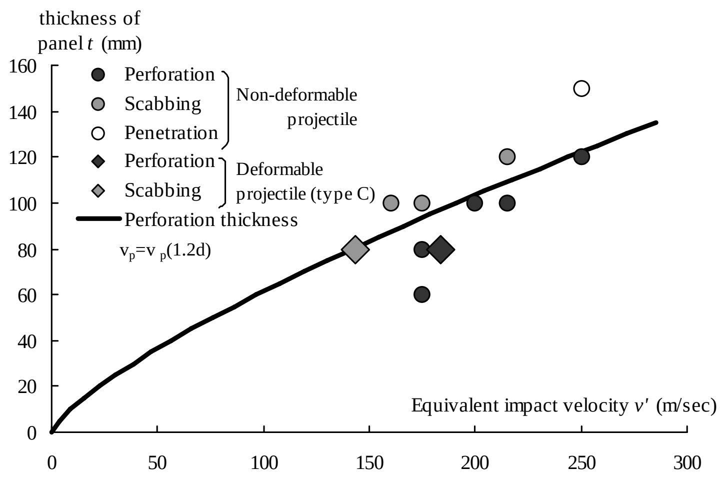

Fig.17 – Evaluation of perforation velocity of RC

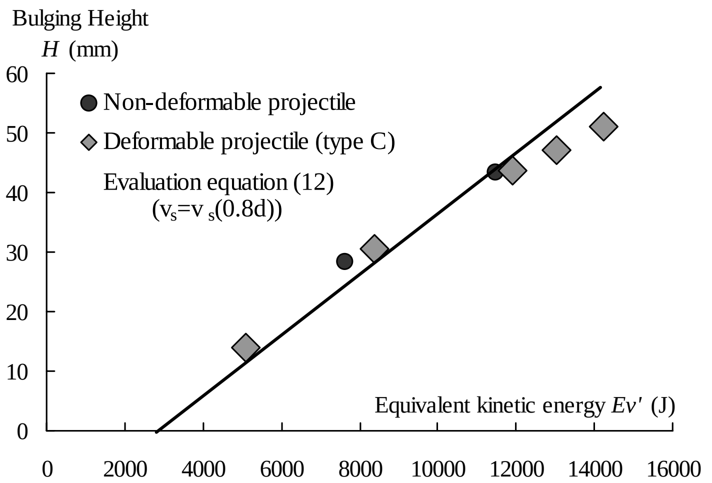

*1 The spacing of stud bolts on steel plate is 100mm.

Fig.18 – Evaluation of bulging height of HSC (t=80mm)

Considering Equation (10) as for the HSC specimens, it is examined that the bulging height of the specimens can be evaluated with the same evaluation equation as a non-deformable projectile. With the evaluation equation using the equivalent kinetic energy E_v', the bulging height can be described as:

$$H = \frac{144.4}{\sqrt{T}} \cdot \frac{m(v'-v_s)^2}{2\pi\left(t+\frac{d}{2}\right)^2} \qquad \text{Eq. (12)}$$

Here, $v_s(0.8t)$ was used to evaluate the bulging height.

Figure 18 shows the relationship between the equivalent kinetic energy of projectile E_v' and the bulging height H on HSC with panel thickness of 80mm. In the same way as the evaluation of the perforation velocity for RC, $E_a = 0$ for non-deformable projectile and $E_a = E_a(v)$ for deformable projectile were used in calculation of E_v'. It can be observed from Figure 18 that the test results using deformable projectile can accurately be evaluated with Equation (12). However, there is a difference between the test results and the evaluation using Equation (12), when the equivalent kinetic energy E_v' becomes larger. In this study, data could not be obtained in the compression test of the deformable projectile (type C) after deformation of projectile reached around 70mm, and the absorbed energy of the deformable projectile was modeled with two straight lines (see Figure 14). It is supposed that this is a reason why the relationship between the deformation and the absorbed energy of the deformable projectile could not estimated when the deformation was large.

4. CONCLUSION

This study summarized the results of three types of panel specimens subjected to impact of non-deformable and deformable projectiles. The parameters studied include thickness of the panels and steel plates, the velocity of the projectiles, and the rigidity of projectile. An attempt made to develop a method for quantitative evaluation of relationship between bulging height of steel plate of HSC specimen and velocity of missile projectile is also reported. From the results of the experimental study, the following conclusions can be drawn:

(1) A concrete panel with a steel plate on its rear face has higher impact resistance performance than a reinforced concrete panel. When used on the front face of concrete panel, as opposed to the rear face, a steel plate is less effective at impact resistance.

(2) The relationship between the velocity of projectile and bulging height of the steel plate on the rear face of a concrete panel was evaluated quantitatively with the experimental results, and the evaluation equation for scabbing velocity of a projectile was proposed.

(3) On a reinforced concrete panel and half steel plate reinforced concrete panel, the degree of local damage by impact of a deformable projectile is smaller than that by impact of a non-deformable projectile.

(4) The kinetic energy of a non-deformable projectile was regarded as equivalent to subtracting absorbed energy by deformation of deformable projectile from total kinetic energy of deformable projectile. Regarding deformable projectiles, the perforation velocity for a reinforced concrete panel and the bulging height for a half steel plate reinforced concrete panel could be evaluated with the evaluation equation for non-deformable projectiles.

REFFERENCE

[1] W. S. Chang, Impact of Solid Missile on Concrete Barriers, Journal of the Structural Division, ASCE, Vol.106, No.ST2, pp.257-271.

[2] NDRC 1946, Effects of Impact and Explosion, Summary Technical Report of Division 2, Vol.1, National Defense Research Committee, Washington DC.

[3] P. Degen, Perforation of Reinforced Concrete Slabs by Rigid Missiles, Journal of the Structural Division, ASCE, Vol.106, No.ST7, 1980, pp.1623-1642

[4] A. Haldar, Energy-balanced approach to evaluate local effects of impact of non deformable missiles on concrete structures, 8^{th} SMiRT J6/3, 1985

[5] J. Hashimoto, K. Takiguchi, K. Nishimura, and M. Tsutsui, Behavior of RC Panels Retrofitted with Aramid Fiber Sheets to Missile Impact, 18^{th} SMiRT, J05/5, 2005.